CrossMark

Straightforward Downsizing of Inclusions in NiTi Alloys: A New Generation of SMA Wires with Outstanding Fatigue Life

Alberto Coda[1] · Andrea Cadelli[1] · Matteo Zanella[1] · Luca Fumagalli[1]

Abstract One of most debated aspects around Nitinol quality is microcleanliness, nowadays considered as the main factor affecting fatigue life. Recent results demonstrate that fatigue is undoubtedly associated with inclusions which can act as crack initiators. However, type, size, and distribution of such particles have been observed to strongly depend on Ni/Ti ratio as well as melting and thermo-mechanical processes. Therefore, if a general reduction of non-metallic inclusions is expected to generate a beneficial effect in improving lifetime of Nitinol, on the other hand this necessarily involves a hard review of both material melting and processing. In this work, the characterization of the fatigue behavior of SMA wires with diameter below 100 μm is presented. The wires were prepared by a peculiar, non-standard combination of melting and thermo-mechanical processes (Clean Melt technology). Thermo-mechanical cycling was carried out and the fracture surfaces of all failed wires were investigated by scanning electron microscopy. A robust set of data was collected and analyzed by using the statistics of extremes. Results clearly demonstrate that in the new NiTi Clean Melt alloy the maximum inclusion size and area fraction are significantly reduced compared to standard Nitinol. This offers meaningful improvement in fatigue resistance over standard wires.

Keywords NiTi shape memory wires · Fatigue · Inclusions · Extreme value

✉ Alberto Coda
  alberto_coda@saes-group.com

[1] SAES Getters S.p.A, 20020 Lainate, MI, Italy

Introduction

NiTi-based shape memory alloys (SMA) are functional materials with a multitude of properties interesting for technological applications. These properties depend on the peculiar deformation mechanisms, accounting for the shape memory effect, the superelastic behavior and the damping capacity of these materials [1]. SMAs are used in different fields, like thermo-mechanical devices [2], anti-loosening systems [3], biomedical applications [4], mechanical damping systems, and in some cases employed for large-scale civil engineering structures [5]. NiTi shows a very good combination of properties, especially in terms of energy density and a large amount of recoverable strain compared to other actuator principles. The obvious simplicity of mechanical design and minimum number of moving parts is amazing for an actuator and make SMAs particularly attractive for microsystems applications. Considerable progress has been made thanks to the integration and miniaturization of sensors, control electronics and the implementation of intelligence using integrated microcontrollers and specific softwares.

However, there are several design criteria that must be controlled to guarantee a widespread diffusion of SMAs to technological fields. For instance, SMAs display a narrow dependence of the shape-memory related properties, like transition temperatures, on their actual composition. For this reason, a great care in the production steps, mainly based on melting and casting processes, is required. Another design criterion lies in the strong influence of thermo-mechanical history on their properties. This may disclose interesting perspectives of application to smart devices in which different aspects of the shape memory phenomenology, like one- and two-way shape memory effect, pseudoelasticity, damping capacity, etc., are used.

Currently, studies are mainly devoted to some aspects related to the material quality and behavior enhancement. Among these, the improvement of thermo-mechanical fatigue represents with no doubt the most important one [6].

Fatigue of SMAs is related to microcleanliness [7]. Microcleanliness of NiTi alloys is rated by the presence of non-metallic inclusions and porosity. The size and distribution of inclusions can play a critical role in affecting the fatigue behavior and the quality of NiTi alloys used in components or products [8]. Typical non-metallic inclusions are carbides (TiC) and oxides ($Ti_4Ni_2O_x$). Through the diligence of the alloy manufacturers, virtually all inclusions in NiTi alloys are indigenous. The type of inclusions, the amount, and the size distribution depend on the raw materials, the melting method, and the thermo-mechanical processes used in making wrought product. The indigenous inclusions are uniformly distributed on a macroscopic scale but segregated on a microscopic scale [9].

The reduction of both size and amount of inclusions is key to increase lifetime of NiTi-based SMA alloys. The benefits of high purity NiTi alloys are yet to be completely quantified. There is evidence that fatigue cracks often nucleate at subsurface inclusions; however, the differences in carbon and oxygen contents between VIM, VIM-VAR, and multiple VAR processes do not result in a measurable difference in fatigue resistance.

Recent results [10–12] claim that fatigue is undoubtedly associated with inclusions which can act as crack initiators. Further works also demonstrate a strong correlation between the fatigue limit and the size of extreme, or maximum inclusions, while the gas impurities amount do not show any evident relationship with the fatigue behavior [13]. However, type, size, and distribution of such particles have been observed to strongly depend on Ni/Ti ratio as well as melting and thermo-mechanical processes. Therefore, if a general reduction of non-metallic inclusions can have a beneficial effect in improving lifetime of Nitinol, on the other hand this necessarily should involve a hard review of both material melting and processing.

From this general background, efforts have been undertaken to reduce the inclusions size, especially for production of very thin shape memory components in which the ratio between wire diameter and inclusion dimension can play a key role and should be maximized in order to guarantee high fatigue performance as required by the new generation of SMA actuators.

In this work, the characterization of the fatigue behavior of NiTi-based shape memory wires with diameter below 100 μm is presented. The wires were manufactured from a new alloy prepared by a unique, non-standard combination of melting and thermo-mechanical processes (Clean Melt technology). The "improved" wires were thus compared with standard materials.

Experimental

SmartFlex® trained wires (Ti 51.0 ± 0.05 at.% $A_s = +95$ °C) with diameter of 25, 76, and 100 μm were prepared with standard VIM-VAR approach and with a new combination of melting and thermo-mechanical process, modified to have smaller inclusions size and area fraction (Clean Melt technology).

Drawing recipe, final cold work ($35\% \pm 10$), surface finish (standard commercial light amber), straight annealing, and training procedures were kept constant and similar to the standard production to neutralize as much as possible secondary effects on functional and fatigue behavior.

Minor Carbon and Oxygen concentrations were detected on ingots by LECO analyzers, using the combustion infrared absorption method as per suggestions of standard practice ASTM F2063-12 [14]. The transformation temperatures were measured at ingot level by differential scanning calorimetry (DSC), as prescribed by the ASTM F2004-05 [15].

The inclusions analysis was carried out in the longitudinal direction of semi-finished hot worked coils ($\emptyset = 6.35$ mm) according to a consolidated internal procedure described by Sczerzenie et al. [16] and following the guidelines indicated within ASTM F2063-12. In particular, the samples were taken from head, center, and tail of full size production spools. Metallographic centerline samples of the materials were prepared by standard practice and analyzed by scanning electron microscopy (SEM). The analysis was carried out by scanning the length of each sample in three regions of the cross section: the centerline, the mid-radius, and the near edge lines. Nine fields of view and over one hundred particles per sample were analyzed.

The shape memory behavior of wires was characterized by uniaxial constant force thermal cycling (UCFTC) under different loading conditions (from 100 to 400 MPa) in a special equipment.

Constant force thermal cycling fatigue was conducted on three different wire diameters (25, 76, and 100 μm) by an ad hoc equipment. To perform these tests, the wire is hanged with a weight clamped at the bottom end and heated up by Joule effect under a constant load. A position laser sensor is located at the bottom side of the weight. When a fixed deformation is reached, the current is stopped. The test bench is shown in Fig. 1. To speed-up thermo-mechanical cycling and increase statistics, a stress of 350 MPa and a strain of 3.5% were selected as testing conditions, and a run-out criteria was set at 150 K cycles.

All failed wires were analyzed by SEM. The observation of the fracture surfaces allows to determine whether an inclusion nucleated the crack and, when present, the dimensions of the inclusion at the nucleation site. The distance of the particle from the surface and its shape were also measured in order to properly compensate the particle area as recommended by Murakami [17]. Measurements of inclusions size were expressed in terms of Murakami's $\sqrt{\text{area}}$ parameter. The estimation of maximum defects was conducted with statistics of extremes: in the most simple version, it is based on the block maxima sampling, where only the maximum defects detected on a given area (or volume) are recorded and then analyzed with *Type I extreme value* (also called *largest extreme value or Gumbel*) *distribution* [18].

Results and Discussion

Preliminary checks on chemistry and impurities of the new material were performed at ingot level. Results are summarized in Table 1. As it can be seen, Clean Melt alloy looks aligned with standard VIM-VAR NiTi either as gas impurities and transformation temperatures. This is a confirmation that the Carbon and Oxygen contents cannot be used as suitable indicators to predict the fatigue behavior.

The results of the optimization activity around smaller and lower inclusions material are reported in Fig. 2(a, b), where microstructures of standard NiTi and Clean Melt are compared. Following the indications of ASTM F2063-12
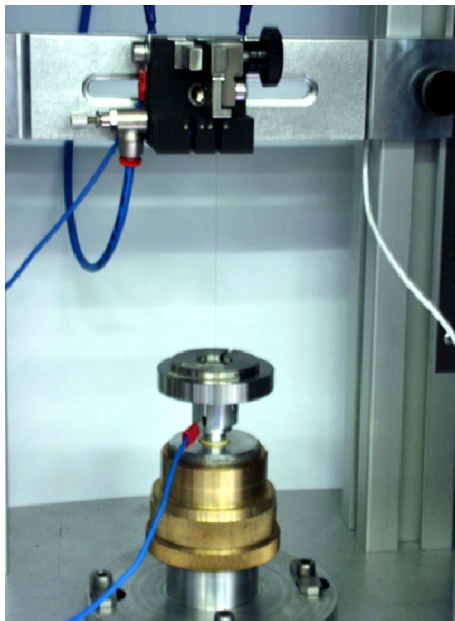
Table 1 Average gas impurities (C and O) contents and A_s temperatures (after full annealing) of standard VIM-VAR and clean melt ingots

Material	Avg. C (ppm)	Avg. O (ppm)	A_s f.a. (°C)
Standard VIM-VAR	< 300	< 300	90 ± 5
Clean melt alloy	280	250	90 ± 5

standard practice, inclusions analysis is typically performed on semi-finished hot worked coil (∅ = 6.35 mm). SEM micrographs show that the main differences between the materials are due to the dimensional and morphological distribution of non-metallic inclusions. In standard NiTi large intermetallic oxide inclusions with stringers and voids formation are often evident, while in Clean Melt NiTi more globular intermetallic oxides are significantly smaller as well as lower in density. In the analysis, no distinction was done between inclusions and voids, but from SEM pictures is clearly evident that in Clean Melt material there are no or very limited voids and smaller inclusions demonstrating that the new melting and hot processing combination can effectively affect the inclusions size and area fraction as well as voids. Table 2 summarizes the results in terms of maximum area fraction and inclusion size as recommended by ASTM F2063-12. The indicated values are the averages calculated from the historical production database of standard coils and from several lots of improved ones. As it can be seen, the maximum inclusions size of about 70 μm in the standard material has been reduced by 5 times in the "improved" one (below 15 μm), whereas the average inclusions size is below 1 μm, with more than 99 percent of the non-metallic particles below 3 μm. Either values of maximum size and area fraction of the new alloy make this material fully compliant to the ASTM F2063-12.

As already anticipated, wires with diameter of 25, 76, and 100 μm were prepared by cold drawing from coils following a standard procedure. Final straight annealing, surface finish, and training were kept constant. The trained wires were thus characterized, first of all, to evaluate their shape memory behavior in terms of transformation temperatures and maximum recoverable strain under different loading conditions. UCFTC curves (under 320 MPa stress) of standard and "improved" wires, reported in Fig. 3, do not display any relevant difference between the two materials. The hysteresis of the Clean Melt is approximately 10% larger than that of the standard material. This difference is typically within the range of the statistical variability of the method. To verify that such small difference does not affect the actuation behavior, the response speed under Joule heating is usually checked. In fact, it is
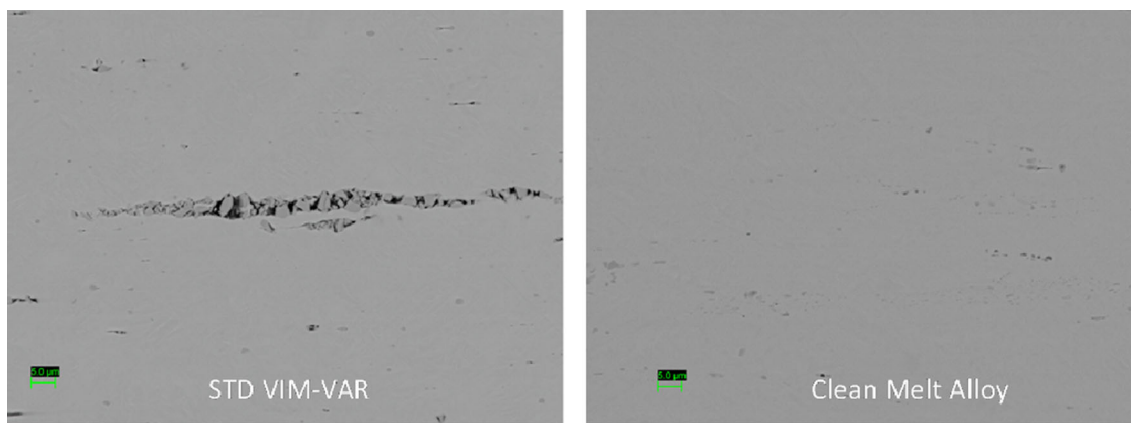

Fig. 1 Test apparatus for functional and fatigue characterization

Fig. 2 SEM micrographs of **a** standard VIM-VAR and **b** Clean Melt alloy at coil level

Table 2 Comparison of inclusion analysis between historical production of standard wires and several lots of improved ones

Hot rolled coil (Φ = 6.35 mm)	Max. inclusions size (µm)	Avg. inclusions size (µm)	Max. area fraction (%)	Percentage (%) of inclusions < 3 µm
STD VIM-VAR	> 70	29	> 4	96
Clean melt alloy	< 15	< 1	< 2	> 99.5

Data are referred to the inclusions analysis performed on semi-finished hot worked coils

very important to know the actuation and relaxation time depending on the different operating conditions. Typically, actuation time varies a little with current, and it is comprised between a minimum value (necessary to the material to complete the transformation) and a maximum (above which there is the risk to overheat the wire). For sake of brevity, these data will not be reported here, but it is worth to underline that no differences in the actuation speed were detected between standard and "improved" wires. So, the new melting and processing strategy does not affect the expected functional behavior of the final wires that appear to be aligned to the standard ones.
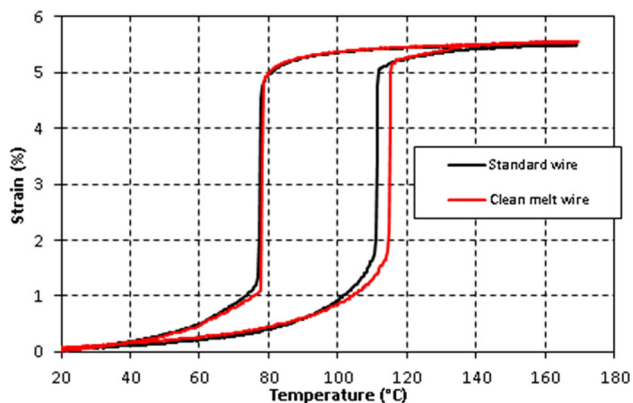
By comparing fatigue data of standard and "improved" wires, it is instead evident how the reduction of inclusions size can have a significantly strong and beneficial impact on fatigue behavior. Looking at Fig. 4, the lifetime of "improved" 25 µm wires (in red) increases of 2–8 times compared to standard material (in black), with a survival probability (at 150 K cycles) of more than 20% in comparison to 0% of standard wires fulfilling the run-out criteria in the selected operating conditions. Moreover, the new material was also tested at higher strains (3.8 and 4%, respectively) working properly and withstanding these
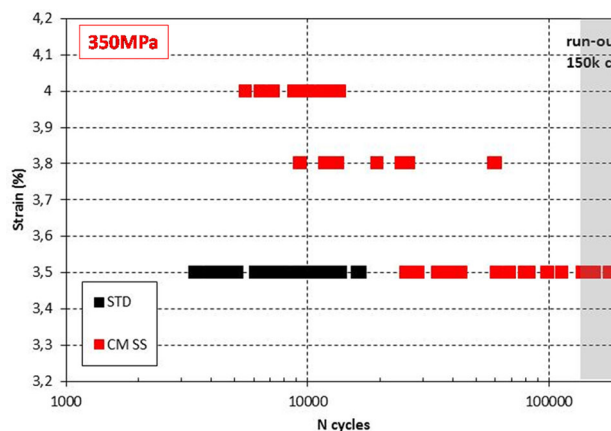

Fig. 3 Uniaxial constant force (320 MPa) thermal cycling (UCFTC) of standard and "improved" wires

Fig. 4 Fatigue data of 25 µm standard and improved wires at 350 MPa constant stress

more aggressive conditions with a better or even equal lifetime than standard material. Table 3 summarizes the results of fatigue testing for 25, 76, and 100 μm wires, both standard and "improved," in terms of average number of cycles and minimum number of cycles to failure. Despite a still poor statistical set of data for 76 and 100 μm wires, differences are clearly evident between standard and "improved" material, confirming the robustness of results obtained on 25 μm wires.

Finally, fracture surfaces of all failed wires were investigated according the prescriptions of ASTM E2283-03 [19] and results analyzed by *extreme value statistics (EVS)*. This sampling strategy can be applied very simply to the inclusion detected at the origin of fractures since we expect that failures have occurred at the largest inclusion present in the most stressed volume.

From SEM analysis, it comes out that all the fractures nucleate from an inclusion. In particular, for Ti-rich alloy, 100% of fractures nucleate from an intermetallic oxide.

According to EVS, the cumulative probability of the particles diameter for each material should follow the Gumbel distribution function [18]:

$$F(x) = \exp\left[-\exp\left(-\frac{x-\lambda}{\delta}\right)\right], \tag{1}$$

where λ and δ, respectively, are the location (63.2 percentile) and the scale parameters. Using Eq. (1), data can be plotted on a *Gumbel probability plot* where the defect inclusions are plotted against the reduced variate $-ln(-ln(P))$, where P are the empirical cumulative probabilities for the different data points. Such a plot is shown in Fig. 5 for extreme inclusions in 25 μm wires of the two different materials. The best-fit distribution, whose parameters have been calculated with the moment's method described by Beretta et al. [20], is plotted on the same graph together with 95% confidence bands. It can be clearly seen that the Gumbel distribution describes quite well the data. According to this figure, samples obtained from materials characterized by different inclusions distributions behave differently under fatigue testing. In particular, the reduction of the maximum (extreme) size as

well as an overall size reduction of non-metallic inclusions has a tremendous effect on the enhancement of the fatigue properties, not only in the high-cycle fatigue region (structural fatigue), but also in the low-cycle fatigue region (where the functional fatigue play a key role). This result also supports the concepts of *extreme value inclusion rating* for the quality control of NiTi-based shape memory materials.

Although thermo-mechanical cycling is an excellent tool for rapidly assessing fatigue performance, the trends presented and discussed in this work may not necessarily be correlated to those that could be observed in finished devices that utilize NiTi SMA wires. The effect of inclusions is clearly demonstrated, but readers should assess fatigue testing on their own devices using the relevant deformation mode and operating conditions.

To further support our conclusions, a statistically relevant number of 25 μm wires were fatigue tested on a different device under less aggressive, but operating-like conditions. The runout criterion in this experimental campaign was fixed at 1 million of cycles. Table 4 summarizes results for standard and "improved" wires under 300 MPa stress and maximum recoverable strain (about 5%). Also in this case, it can be observed and measured how much better the "improved" wires perform against the standard with an average lifetime of few thousands cycles for standard wires and more than half a million for "improved" ones (over 100 times difference), respectively.

Conclusions

There are several devices in mass production adopting NiTi SMA, especially in automotive and thermostatic applications. A very promising industrial sector is that of miniaturized actuators for consumer electronics where thin wires, in the range 20–100 μm in diameter, are used to produce small- and high-quality actuators.

An example of a SMA device developed using thin SmartFlex® wires is camera module for mobile phones. SMA wires can enable the double function of auto-focus and optical image stabilization (OIS) at the same time. The lens and sensor are tilted together with SMA wire on all four sides of the camera. Both pitch and yaw tilt are measured by a gyroscope moving mechanically attached to the camera and compensated to a zero output by the OIS actuator. With OIS enabled, the lens and sensor tilt inside the camera, but still remain to the image subject giving a sharp image. SMA technology allows a fast and accurate stabilization of the new-generation big lenses and glass lenses for high-performance mobile cameras. The SMA device here described represents only one example clearly demonstrating that the future directions for successful

Table 3 Fatigue results for 25, 76, and 100 μm standard and "improved" wires

Wire	N° tests	$\langle N \rangle$	N_{min}
25 μm STD	40	8527	3464
25 μm improved	53	67,616	13,176
76 μm STD	8	13,220	11,116
76 μm improved	8	44,416	26,304
100 μm STD	7	9861	8144
100 μm improved	7	48,998	43,558

Fig. 5 Standard and improved wire Gumbel distributions of extreme inclusions detected and measured at the crack tip of all failed wires
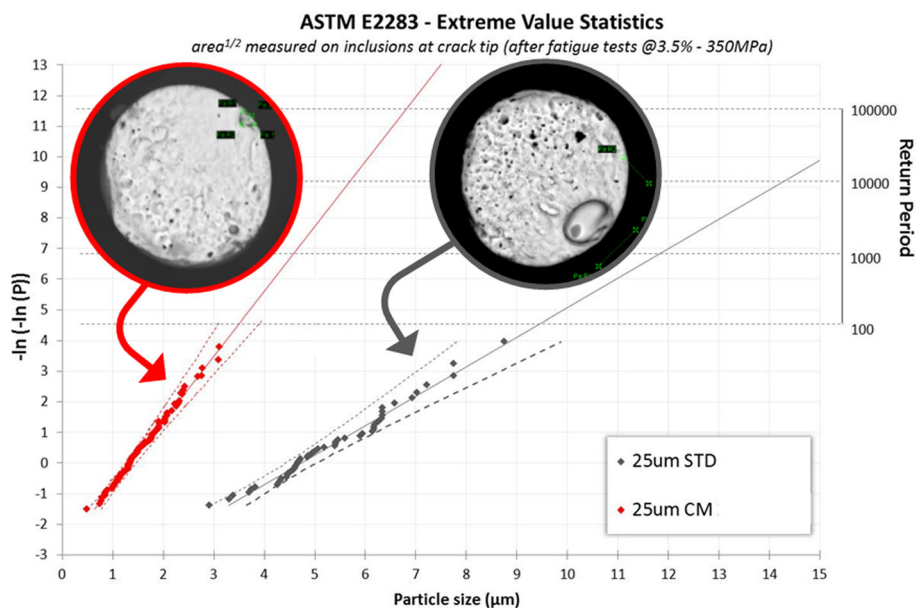

Table 4 Fatigue results for 25 μm standard and "improved" wires in more real conditions

Wire	Stress (MPa)	Recoverable strain	N° test	Avg. N° cycles to failure	Minimum N° cycles to failure
STD SmartFlex®	300	Max	27	6176	3550
Improved wire	300	Max	> 80	> 500,000	40,000

exploitation of the SMA technology seem to go towards miniaturization, integration and multifunctional embedded systems.

The shape memory wires used in such devices have to guarantee high performance and reliability as well as very long lifetime. The "improved" SmartFlex® wires manufactured from Clean Melt alloy and presented in this work show a perfect agreement with the standard ones in terms of chemistry, microstructure and functional properties, at the same time coupled with an outstanding fatigue behaviour (5–100X), thus opening the doors to a new generation of products for micro-actuation.

References

1. Duerig TW, Melton KN, Stockel D, Wayman CM (1990) Engineering aspects of shape memory alloys. Butterworth-Heinemann, London
2. Ionaitis RR (2000) Directly acting pipeline SM devices for nuclear power plants. Mat Sci For 327–328:51–54
3. Zhang X, Nie J, Hou G (2000) Development of anti-loosening nuts using shape memory alloys. Mat Sci For 327–328:35–38
4. Mantovani D (2000) Shape memory alloys: properties and biomedical applications. JOM 52(10):36–44
5. Adachi Y, Unjoh S, Kondoh M (2000) Development of a shape memory alloy damper for intelligent bridge systems. Mat Sci For 327–328:31–34
6. Adler PH et al (2007) Martensite transformations and fatigue behavior of nitinol. J ASTM Int 4:3–16
7. Pelton AR (2011) Nitinol fatigue: a review of microstructures and mechanisms. JMEPEG 20:613–617
8. Wong S, Lin ZC, Tahran A, Boylan J, Pike K, Kramer-Brown P (2009) An investigation of factors impacting nitinol wire fatigue life. J ASTM Int 6:99–107
9. M. Reinoehl et al. (2000) The influence of melt practice on final fatigue properties of superlesatic NiTi wires. In: SMST-2000 proceedings international conference on shape memory and superelastic technologies, p 397–403
10. Rahim M et al (2013) Impurity levels and fatigue lives of pseudoelastic NiTi shape memory alloys. Acta Mater 61(10):3667–3686
11. Steegmuller R et al (2014) Analysis of new nitinol ingot qualities. J Mater Eng Perform 23:2450–2456
12. Launey M et al (2014) Influence of microstructural purity on the bending fatigue behavior of VAR-Melted superelastic nitinol. J Mech Behav Biomed Mater 34:181–186
13. Urbano M et al (2015) Inclusions size-based fatigue life prediction model of NiTi alloy for biomedical applications. Shape Mem Superelast 1(2):240–251
14. Standard specification for wrought nickel-titanium shape memory alloys for medical devices and surgical implants, ASTM F2063-12 (2012)
15. Standard ASTM (2004) Standard test method for transformation temperature of nickel-titanium alloys by thermal analysis. ASTM Standard 5:1–4

16. Sczerzenie F, Vergani G, Belden C (2012) The measurement of total inclusion content in nickel–titanium alloys. J Mater Eng Perform 21:2578–2586

17. Murakami Y (2002) Metal fatigue: effect of small defects and nonmetallic inclusions. Elsevier, Amsterdam

18. Murakami Y, Beretta S (1999) Small defects and inhomogeneities in fatigue strength: experiments models and statistical implications. Extremes 2:123–147

19. Standard practice for extreme value analysis of nonmetallic inclusions in steel and other microstructural features, ASTM E2283-08 (2014)

20. Beretta S, Murakami Y (1998) Statistical analysis of defect for fatigue strength prediction and quality control of materials. Fatigue Fract Eng Mater Struct 21:1049–1065